Available online at www.sciencedirect.com
ScienceDirect
Ceramics International 37 (2011) 2297–2303
CERAMICS INTERNATIONAL
www.elsevier.com/locate/ceramint

Preparation of silica xerogel with high silanol content from sodium silicate and its application as CO_2 adsorbent

Thongthai Witoon [a,b,*], Naradon Tatan [a], Priwit Rattanavichian [a], Metta Chareonpanich [a,b]

[a] National Center of Excellence for Petroleum, Petrochemicals and Advance Material, Department of Chemical Engineering, Faculty of Engineering, Kasetsart University, Bangkok 10900, Thailand

[b] Center for Advanced Studies in Nanotechnology and its Applications in Chemical Food and Agricultural Industries, Kasetsart University, Bangkok 10900, Thailand

Received 13 January 2011; received in revised form 10 March 2011; accepted 14 March 2011
Available online 23 March 2011

Abstract

In this study, silica xerogels with high silanol content were synthesized by using sodium silicate as low-cost silica source in the presence of hydrochloric acid and acetic acid via sol–gel process for CO_2 adsorption purpose. The effect of amount of acetic acid on the surface and structural properties of silica xerogel was investigated. Fourier transform infrared spectroscopy (FTIR) and thermal gravimetric analysis (TGA) revealed that the silanol groups existed on the surface of silica xerogel products and their concentration increased with increasing the amount of acetic acid. The BET surface area and total pore volume of the silica xerogel prepared using 6 mL of acetic acid (MMS-6) were found to be 1021 m^2/g and 0.72 cm^3/g, respectively. The pore structure of silica xerogel products consisted of the interparticle voids between the nanoparticles aggregates, and the interconnected wormhole microporous structure. The latter pore structure was more uniform on increasing the amount of acetic acid. CO_2 adsorption/desorption measurements were carried out using TGA unit with high purity CO_2 (99.999%). The highest CO_2 sorption capacity (83.6 $mg_{CO2}/g_{sorbent}$) was obtained with MMS-6 product. Thermal swing adsorption studies showed that the silica xerogel products exhibited strongly reversible CO_2 adsorption capacity and stable during 5-repeated cycle of adsorption/desorption experiment at 35 °C.

Keywords: Silica xerogel; Acetic acid; Water glass; Sol–gel process; CO_2 adsorption

1. Introduction

The increase of CO_2 emissions into the earth's atmosphere has raised serious concerns about global warming [1–3]. The combustion of fossil fuels is one of the major sources of the greenhouse gas CO_2. However, fossil fuels supply more than 80% of the world's energy requirements [4]. It is therefore essential to develop technologies that will allow us to utilize the fossil fuels while reducing the emissions of greenhouse gases [5]. Generally, there are three steps in CO_2 management involving separation, transportation and sequestration [2]. The key point for the sequestration is the removal of CO_2 from flue gases by a gas separation process prior to its release to the atmosphere.

Various strategies for CO_2 capture technologies including absorption, adsorption, cryogenics, membranes, and so forth, have been proposed and investigated [1,2,6]. Among these techniques, adsorption is one of the most promising approaches as it can reduce the cost associated with the capture step [1–3]. Generally, the high CO_2 capture capacity, low cost materials, high selectivity and stable adsorption capacity after several cycles are the main properties of the CO_2 adsorbent. Several porous materials such as zeolite 4A, zeolite 13X, ZSM-5, activated carbons, and porous silica have been considered for low temperature CO_2 capture [5,7–10]. The CO_2 capture capacity of these materials, generated by physisorption induced by ion-quadrupole interaction (zeolites), van der Waals forces (activated carbons), and hydrogen bonding between residual hydroxyl

* Corresponding author at: National Center of Excellence for Petroleum, Petrochemicals and Advance Material, Department of Chemical Engineering, Faculty of Engineering, Kasetsart University, Bangkok 10900, Thailand.
Tel.: +66 2579 2083; fax: +66 2561 4621.
E-mail address: fengttwi@ku.ac.th (T. Witoon).

0272-8842/$36.00
doi:10.1016/j.ceramint.2011.03.020

groups and CO_2 (porous silica). Therefore, the increase of concentration of silanol groups on the silica surface could possibly promote the CO_2 adsorption capacity.

The sol–gel process is an attractive method to synthesize porous materials with controllable surface and structural properties. Generally, the sol–gel process consists of hydrolysis and condensation of alkoxide precursor. After evaporating the pore liquid of the as-synthesized silica gel at atmospheric pressure, the obtained porous silica is called silica xerogel. Although the necessary chemistry is simple, variation of one or more parameters including pH of solution, reaction temperature and water/silica ratios can dramatically affect the microstructure of the resulting silica xerogels [11,12].

In this work, we attempted to synthesize silica xerogel with high uniform porous structure and high surface concentration of silanol groups using water glass (sodium silicate) as low-cost silica source instead of tetraethyl orthosilicate (TEOS). Hydrochloric acid and acetic acid were used as the catalysts for the hydrolysis and condensation reaction. The effect of acetic acid amount on the surface and structural properties of the silica xerogel products was investigated by thermogravimetric analysis (TGA), Fourier transform infrared (FTIR) spectroscopy, nitrogen adsorption–desorption measurement, scanning electron microscopy (SEM), and transmission electron microscopy (TEM). CO_2 adsorption capacity of each sample was measured by gravimetric method at different adsorption temperatures. Durability test using selected silica xerogel product was also conducted.

2. Experiment

2.1. Synthesis of silica xerogel

Silica xerogels were prepared by sol–gel method based on hydrolysis and condensation reaction of sodium silicate. In a typical synthesis process, 4.5 g sodium silicate which was supplied from Thai Silicate Chemicals Co., Ltd. ($Na_2Si_3O_7$: 27 wt.% SiO_2, 4 wt.% NaOH) was introduced into 70 mL deionized water under stirring for 5 min. Then, acetic acid solution was gradually added into the sodium silica solution. The different amounts of acetic acid solution including 0, 2, 4, and 6 mL were employed. Afterwards the pH of solution was adjusted to 2 using 2 M hydrochloric acid. The solution was stirred continuously at 40 °C for 24 h, and then the obtained solution was aged in the Teflon-lined autoclave at 100 °C for 24 h. The obtained gel was consecutively filtered, washed several times with distilled water, washed with 100 mL absolute ethanol, and dried at 105 °C for 12 h. The dried silica xerogels were a bulk form and were crushed to be a powder form prior to CO_2 adsorption measurement. All silica xerogel products were calcined in air at 200 °C for 4 h with a heating of 1 °C/min to remove physical and chemical adsorption of water molecules.

2.2. Characterization of silica xerogel

The amount of silanol groups adsorbed on the surface of silica xerogel was investigated by using simultaneous DTA–TGA analyzer (TA instrument, SDT2960 simultaneous DTA–TGA Universal 2000) in air at a heating rate of 10 °C/min. The functional groups on the surface of silica xerogel were examined by using Fourier transform infrared spectroscopy (Perkin Elmer System 2000 using KBr pellet). Nitrogen isotherms of silica xerogel products were measured at −196 °C using a Quantachrome Autosorb-1 C instrument. Prior to N_2-physisorption measurements, the products were degassed at 200 °C for 12 h. The adsorption isotherms were run at $10^{-5} < P/P_0 < 1.0$. Using the nitrogen adsorption data, the specific BET (S_{BET}) was estimated for P/P_0 values between 0.05 and 0.30. Various methods were used to evaluate the characteristic of microporosity since it is an important factor on the adsorption process of which is the fundamental aim of this work. Micropore size distribution and micropore volume were obtained from the extended application of the *V–t* plots called MP method [13] and nonlocal density functional theory (NLDFT) method [14]. The micropore analysis was also carried out using relative pressure range of $10^{-4} < P/P_0 < 10^{-2}$ of the theory of Dubinin (DR plot) [15]. Mesopore size distribution was calculated by Barrett–Joyner–Halenda (BJH) method [15]. The total pore volume and the volume of meso-micropores were obtained from adsorption data at P/P_0 of 0.99 and P/P_0 of 0.95, respectively [16]. The surface morphology and the pore structure of silica xerogels were analyzed by using field emission scanning electron microscopy (FE-SEM: JEOL JSM-6301F with Au-coated, operated at 20 keV) and transmission electron microscopy (TEM: JEOL JEM-2010 microscope with the acceleration voltage of 200 kV). In order to prepare the sample for TEM analysis, the nanostructured silica products were suspended in ethanol and dried at room temperature on a copper grid coated with a carbon film.

2.3. CO_2 adsorption/desorption measurements

CO_2 adsorption/desorption measurement was performed for all silica xerogel products by using SDT2960 simultaneous DTA–TGA Universal 2000. A 20 mg of sample was loaded into an alumina sample pan. Prior to any CO_2 adsorption/desorption experiment, the sample was first activated by heating in a flow of Ar (99.99%) at a rate of 10 °C/min from room temperature to 110 °C in order to remove pre-adsorbed carbon dioxide and water and then cooled down to a given temperature. Subsequently, pure CO_2 (99.999%) with a flow rate of 40 mL/min was introduced into the system while the change in the sample weight was recorded. The CO_2 adsorption runs were conducted at three different temperatures including 35 °C, 55 °C and 75 °C. When the sample weight was constant, CO_2 was then desorbed by heating in a flow of Ar (99.99%) at a rate of 10 °C/min to 110 °C. The same experiment was repeated 5 times in order to investigate the reversible and stable CO_2 adsorption–desorption performance.

3. Results and discussion

Fig. 1 shows TGA patterns of as-synthesized silica xerogels prepared using different amounts of acetic acid. It was found

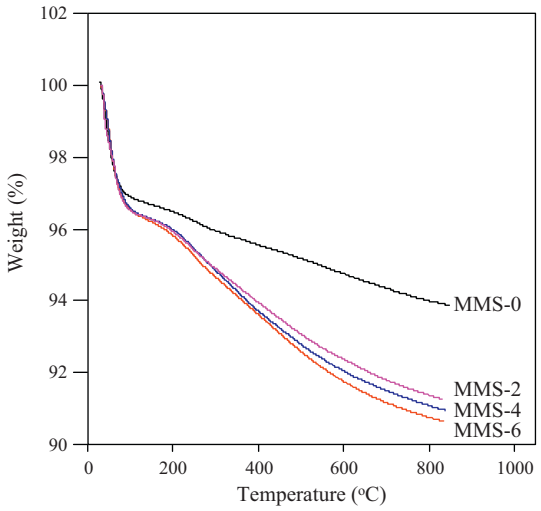

Fig. 1. TGA patterns of dried silica xerogel prepared using different amounts of acetic acid.

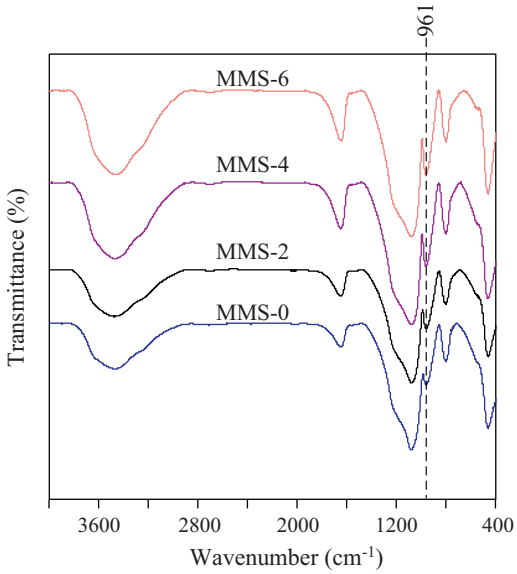

Fig. 2. FTIR spectra of calcined silica xerogel prepared using different amounts of acetic acid.

that the TGA patterns of silica xerogels consisted of three steps of weight losses at the temperature below 100 °C, between 100 and 200 °C and above 200 °C. The first and the second steps were attributed to physically adsorbed and chemically adsorbed water molecules, respectively. The last step was due to the loss of water by means of the condensation of single, geminal, and vicinal silanols [11,17]. The weight loss caused by the condensation of silanol groups was increased from 2.8 to 5.8% when the amount of acetic acid was increased from 0 to 6 mL.

Fig. 2 shows the IR spectra of the silica xerogels calcined at 200 °C. The strong band around 1100 cm^{-1} and small bands around 780 and 460 cm^{-1} represented the characteristics of Si–O–Si groups [18]. The broad band between ~3800 and 3050 cm^{-1} is assigned to the O–H stretching mode [19]. The shoulder at ~961 cm^{-1} is also related to residual silanol groups, resulting from a stretching motion of oxygen atoms not bridging two Si atoms, with contributions from Si–O– and Si–OH vibrations [19]. It was found that all silica xerogels have a very similar chemical nature. However, it is clearly seen that the intensity of the band (961 cm^{-1}) related to the existence of silanol groups increases with the volume of acid acetic

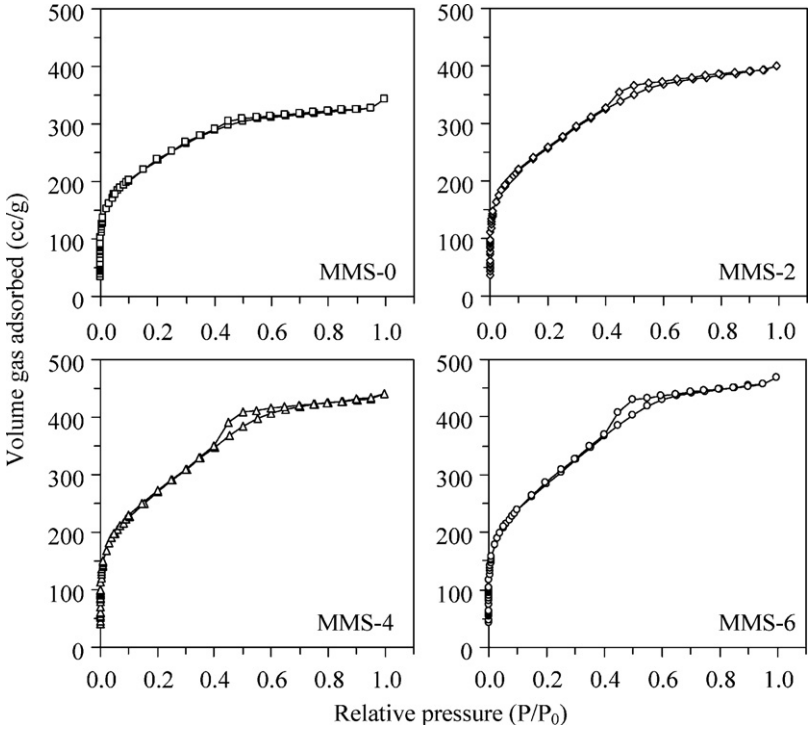

Fig. 3. N_2 sorption isotherms of silica xerogel products prepared using different amounts of acetic acid.

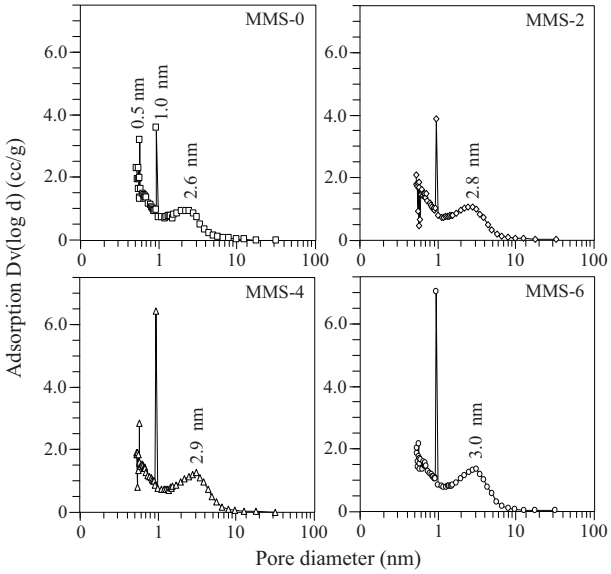

Fig. 4. Pore size distribution of silica xerogel products prepared using different amounts of acetic acid.

employee. This result was in very good agreement with the TGA result regarding the weight loss above 200 °C and therefore it could be concluded that the increase in the amount of acetic acid could increase the amount of silica groups on the surface of silica xerogels.

The N_2 adsorption–desorption isotherms of the silica xerogels calcined at 200 °C are shown in Fig. 3. Without the addition of acetic acid (MMS-0), the microporous silica xerogel of type I isotherm was obtained. With the addition of acetic acid (MMS-2, MMS-4, and MMS-6), the characteristics of microporous–mesoporous materials confirmed by the type I–IV composite isotherms were found. The hysteresis loop of silica xerogels was clearly observed when the larger amount of acetic acid was applied. The pore size distributions of silica xerogels calculated by BJH adsorption method are shown in Fig. 4. It was found that the pore size distribution of silica xerogel prepared without the addition of acetic acid showed the multimodal mean pore diameter of 0.5 nm, 1.0 nm and 2.6 nm. With increasing the amount of acetic acid, the existence of smallest pore size (0.5 nm) was decreased while the medium pore size (1.0 nm) was sharper than that of MMS-0, indicating the highly uniform pore structure. Moreover, the large pore (2.6 nm) was slightly shifted towards larger size (3.0 nm) at the highest acetic acid amount (MMS-6).

The micropore size distributions calculated by NLDFT (a) and MP (b) methods are given in Fig. 5. The micropore size distribution obtained by NLDFT method showed a similar trend (the same multimodal mean pore diameter of 0.72 nm, 1.41 nm, 1.69 nm and 2.6 nm) for all silica xerogels. Increasing amount of acetic acid significantly increased the area under the micropore size distribution curve in the range of 2.4–5.0 nm, indicating a significantly extended micropore volume. The micropore dimensions of all silica xerogels obtained by MP method exhibited unimodal pore distribution of which shifted to larger pore diameter when the amount of acetic acid was increased.

The structural properties of silica xerogels prepared using different amounts of acetic acid are given in Table 1. It was clearly observed that the BET surface area, micropore surface area, micropore volume, total pore volume and average pore diameter of silica xerogel were significantly increased with increasing amount of acetic acid. Insignificant difference of micropore surface areas estimated by MP and DR methods was observed, whereas micropore volumes calculated by MP method were much than those calculated by DR methods. Based on the NLDFT and MP methods, approximately 90% of the BET surface area was related to the micropore surface area.

The surface morphology and pore structure of the representative silica xerogel (MMS-6) are investigated by SEM and TEM shown in Figs. 5 and 6, respectively. SEM images at low and high magnification revealed the smooth and dense surface of MMS-6 caused by an aggregation of fine silica nanoparticles. TEM image at low magnification presented disconnected mesopores several nanometers in size, which exist in the interparticle spaces of many overlapped particles. It was observed that the large pores (2.6–3.0 nm) obtained by N_2-physisorption were related to the aggregation of these nanoparticles, moreover, these nanoparticles also contributed the external surface area which was the difference between

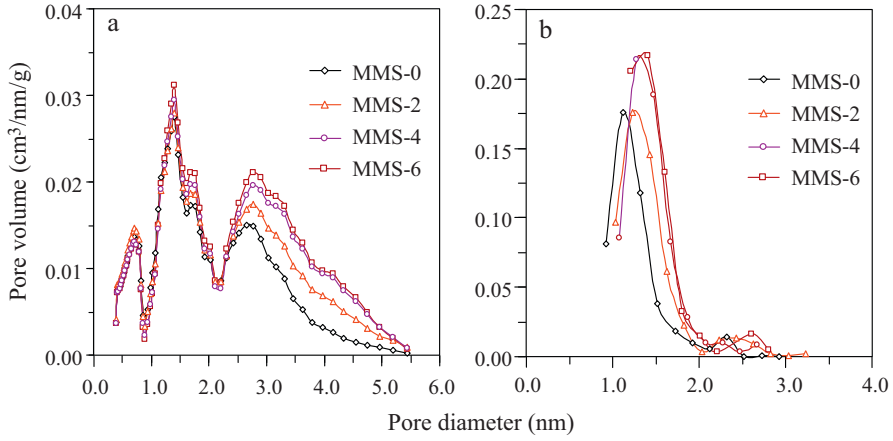

Fig. 5. Pore size distribution of silica xerogel products calculated by: (a) NLDFT method and (b) MP method.

Table 1
Structural properties of silica xerogel.

Sample[a]	Specific surface area (m^2/g)			Pore volume (cm^3/g)					Average pore diameter (nm)		
	S_{BET}	$S_{micro,MP}$	$S_{micro,DR}$	$V_{micro,NLDFT}$	$V_{micro,MP}$	$V_{micro,DR}$	$V_{micro+meso}$	V_{total}	d_{NLDFT}	d_{MP}	d_{BJH}
MMS-0	830	767	774	0.45	0.46	0.28	0.50	0.53	1.41	1.12	2.56
MMS-2	916	847	833	0.54	0.55	0.30	0.61	0.62	1.43	1.23	2.70
MMS-4	967	907	862	0.60	0.63	0.31	0.67	0.68	1.54	1.27	2.82
MMS-6	1021	918	903	0.63	0.64	0.32	0.71	0.72	1.68	1.41	2.84

[a] Silica xerogel products were designated as MMS-*X* where *X* is the amount of acetic acid.

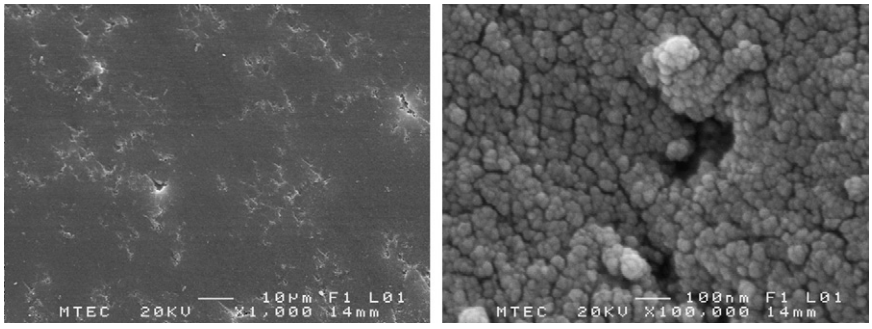

Fig. 6. SEM images of MMS-6 at low and high magnifications.

BET surface area and micropore surface area. TEM image at high magnification revealed interconnected wormhole microporous with highly uniform structure.

In this study, silica xerogels were prepared by the hydrolysis and condensation reaction of sodium silicate precursor in the presence of hydrochloric acid and acetic acid catalysts. It is known that the hydrochloric acid could easily promote the formation of highly reactive silanol species to form siloxane [20]. However, the use of acetic acid catalyst might delay the siloxane formation because several different intermediate pathways could competitively occur [20]. Moreover, acetic acid could stabilize the silanol groups by preventing further condensation of silanol–silanol groups [21]. Therefore, the high concentration of silanol functional groups remained on the surface of silica xerogels which were activated using acetic acid.

Fig. 7(a) shows the consecutive CO_2 adsorption–desorption result for MMS-6 at three different temperatures (35 °C, 55 °C and 75 °C). The weight gain seen in the TGA plot during a flow of CO_2 was calculated as CO_2 adsorption capacity. The initial weight of the sample was considered as 100%, and after preliminary activation by heating in a flow of Ar (99.99%) at a rate of 10 °C/min (until 110 °C), a weight loss of ca. 3.5 wt.% was observed and can be attributed to the removal of moisture content. Following this, the sample was cooled to 35 °C and pure CO_2 (99.999%) was introduced into the system at a flow rate of 40 mL/min, while the increase in the weight of the sample was recorded. The CO_2 adsorbed MMS-6 was subsequently regenerated at 110 °C by purging Ar gas until the weight of sample became constant, implying complete CO_2 desorption. The same cycle was repeated at the adsorption temperatures of 55 °C and 75 °C, consecutively. As shown in

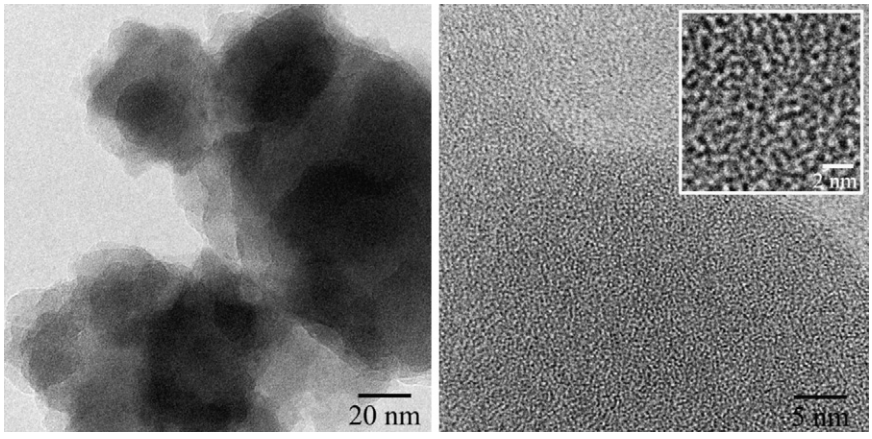

Fig. 7. TEM images of MMS-6 at low and high magnifications.

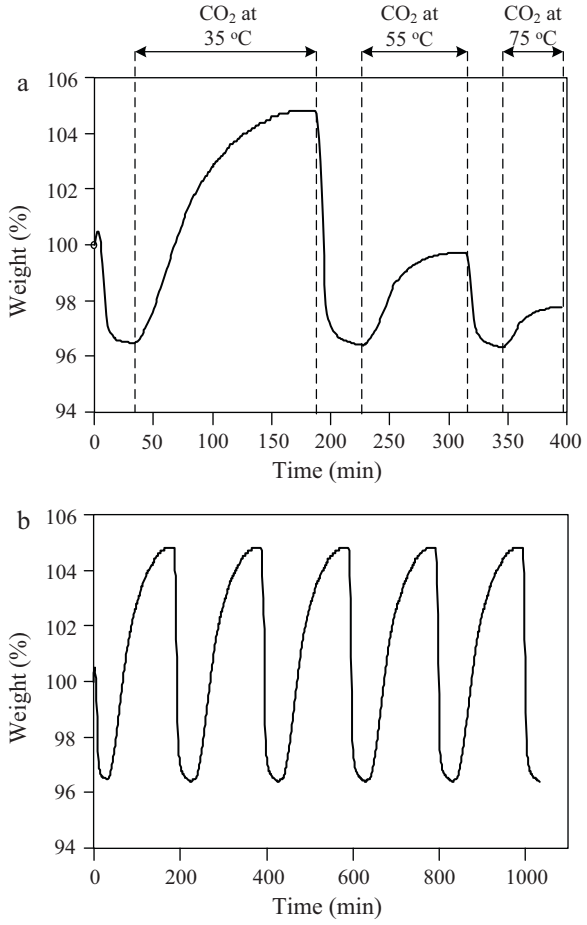

Fig. 8. CO_2 adsorption on MMS-6: (a) continuous CO_2 adsorption at 35 °C, 55 °C and 75 °C and (b) recycle runs of CO_2 adsorption/desorption of MMS-6 at 35 °C.

Fig. 7(b), the MMS-6 product demonstrated a strongly reversible and stable CO_2 adsorption–desorption performance during 5 repeated runs at 35 °C.

Fig. 8 shows the effect of adsorption temperature on CO_2 capture capacity for all samples (MMS-0, MMS-2, MMS-4, and MMS-6). It can be clearly seen that the CO_2 capturing capacity was increased with the amount of acetic acid used to form silica xerogels, since increased use of acetic acid corresponds to more highly uniform pore structure and a high silanol content. The highest CO_2 sorption capacity (83.6 $mg_{CO2}/g_{sorbent}$) was obtained in the case of MMS-6 product. However, differences between the CO_2 sorption capacities of the silica xerogel products at high adsorption temperatures were found to be insignificant. This observation could be explained as follows: the high adsorption temperature may be attributed to a decrease in the interaction and van der Waals' force between CO_2 and silanol groups on the surface of silica xerogels; as a result, the adsorption capacity was significantly decreased, even though there was a high concentration of silanol groups distributed on the surface of silica xerogels products. Fig. 9

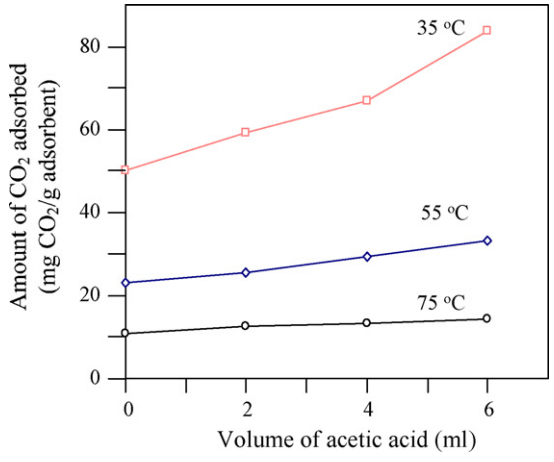

Fig. 9. Comparison of CO_2 adsorption capacity of silica xerogels at different adsorption temperatures.

4. Conclusion

Silica xerogels with high surface area, highly uniform pore structure and high silanol group content were successfully synthesized using low-cost silica source in the presence of hydrochloric acid and acetic acid via sol–gel process. At a low adsorption temperature, the silica xerogel prepared using 6 mL of acetic acid has the highest CO_2 adsorption capacity (83.6 $mg_{CO2}/g_{sorbent}$), due to its high silanol groups content and high uniform pore structure. The CO_2 adsorption capacity was significantly decreased at higher temperature, due to the weak interaction between CO_2 and the surface of silica xerogels. In addition, the silica xerogel product showed strongly reversible and stable CO_2 adsorption–desorption performance in successive cycles.

Acknowledgements

This work is financially supported by the Commission on Higher Education, Ministry of Education (the "National Research University Project of Thailand (NRU)" and the "National Center of Excellence for Petroleum, Petrochemical and Advanced Materials (NCE-PPAM)"). Support from the Kasetsart University Research and Development Institute (KURDI) is also acknowledged.

References

[1] N. MacDowell, N. Florin, A. Buchard, J. Hallett, A. Galindo, G. Jackson, C.S. Adjiman, C.K. Williams, N. Shah, P. Fennell, An overview of CO_2 capture technologies, Energy Environ. Sci. 3 (2010) 1645–1669.
[2] J.D. Figueroa, T. Fout, S. Plasynski, H. McIlvried, R.D. Sricastava, Advances in CO_2 capture technology – the U.S. Department of Energy's Carbon Sequestration Program, Int. J. Greenhouse Gas Control 2 (2008) 9–20.
[3] A.A. Olajire, CO_2 capture and separation technologies for end-of-pipe applications – a review, Energy 35 (2010) 2610–2628.
[4] P. Freund, 2.4 CO_2 removal and deposition. in: K. Heinloth, (Ed.). Springer Materials – The Landolt–Börnstein Database. http://www.springermaterials.com, doi:10.1007/10696439_17.
[5] R.V. Siriwardane, M.-S. Shen, E.P. Fisher, J.A. Poston, Adsorption of CO_2 on molecular sieves and activated carbon, Energy Fuels 15 (2001) 279–284.

[6] G. Xomeritakis, C.Y. Tsai, C.J. Brinker, Microporous sol–gel derived amniosilicate membrane for enhanced carbon dioxide separation, Sep. Purif. Technol. 42 (2005) 249–257.
[7] G. Calleja, J. Pau, J.A. Calles, Pure and multicomponent adsorption equilibrium of carbon dioxide, ethylene, and propane on ZSM-5 zeolites with different Si/Al ratios, J. Chem. Eng. Data 43 (1998) 994–1003.
[8] K.S. Walton, M.B. Abney, M.D. Levan, CO_2 adsorption in Y and X zeolites modified by alkali metal cation exchange, Micropor. Mesopor. Mater. 91 (2006) 78–84.
[9] M. Katoh, K. Sakamoto, M. Kamiyamane, T. Tomida, Adsorption of CO_2 on FSM-type mesoporous silicas, Phys. Chem. Chem. Phys. 2 (2000) 4471–4475.
[10] C. Chen, W.-J. Son, K.-S. You, J.-W. Ahn, W.-S. Ahn, Carbon dioxide capture using amine-impregnated HMS having textural mesoporosity, Chem. Eng. J. 161 (2010) 46–52.
[11] C.J. Brinker, G.W. Scherer, Sol–Gel Science: The Physics and Chemistry of Sol–Gel Processing, Academic Press, New York, 1990.
[12] R. Filipović, Z. Obrenović, I. Stijepović, L.M. Nikolić, V.V. Srdić, Synthesis of mesoporous silica particles with controlled pore structure, Ceramics Int. 35 (2009) 3347–3353.
[13] R.S. Mikhail, S. Brunauer, Some remarks on pore structure analyses, J. Colloid Interface Sci. 52 (1975) 626–627.
[14] A.V. Neimark, P.I. Ravikovitch, A. Vishnyakov, Adsorption hysteresis in nanopores, Phys. Rev. E 62 (2000) R1493–R1496.
[15] S.J. Gregg, K.S.W. Sing, Adsorption, Surface Area and Porosity, Academic Press, New York, 1982.
[16] F.T. Basoglu, S. Balci, Micro-mesopore analysis of Cu^{2+} and Ag^{+} containing Al-pillared bentonite, App. Clay Sci. 50 (2010) 73–80.
[17] T. Witoon, M. Chareonpanich, J. Limtrakul, Effect of acidity on the formation of silica-chitosan hybrid materials and thermal conductive property, J. Sol–Gel Sci. Technol. 51 (2009) 146–152.
[18] I.K. Battisha, A.E. Beyally, S.A.E. Mongy, A.M. Nahrawi, Development of the FTIR properties of nano-structure silica gel doped with different rare earth elements prepared by sol–gel route, J. Sol–Gel Sci. Technol. 41 (2007) 129–137.
[19] T. Karbowiak, M.-A. Saada, S. Rigolet, A. Ballandras, G. Weber, I. Bezverkhyy, M. Soulard, J. Patarin, J.-P. Bellat, New insight in the formation of silanol defects in silicalite-1 by water intrusion under high pressure, Phys. Chem. Chem. Phys. 12 (2010) 11454–11466.
[20] L.T. Arenas, C.W. Simm, Y. Gushikem, S.L.P. Dias, C.C. Moro, T.M.H. Costa, E.V. Benvenutti, Synthesis of silica xerogels with high surface area using acetic acid as catalyst, J. Braz. Chem. Soc. 18 (2007) 886–890.
[21] Y. Liu, W. Ren, L. Zheng, X. Yao, New method for making porous SiO_2 thin films, Thin Solid Films 353 (1999) 124–128.